doi:10.3788/gzxb20174610.1012004

星敏感器测试用微调整机构设计

陈启梦[1,2],张国玉[1,2],张健[1],王哲[3],张宇[4]

(1 长春理工大学 光电工程学院,长春 130022)

(2 吉林省光电测控仪器工程技术研究中心,长春 130022)

(3 长春理工大学 理学院,长春 130022)

(4 航天系统仿真重点实验室,北京 100000)

摘 要:针对高精度星敏感器在地面标定实验中与测试设备准确对接的实际要求,设计一种纳米级星敏感器标定用五维微调整机构.详细分析了光轴对准误差对敏感器测试的影响.为保证对接精确性,提出了搭积型调整架机械结构的设计思想;论述了二维平移和三维调整模块的设计方案;对调整机构进行了仿真建模和力学分析.对设计的微调整机构进行验证性实验,结果表明:位移分辨力可以达到25 nm,角度分辨力可以达到0.1角秒,且稳定性高.设计的微调整机构可以满足星敏感器与测试设备准确对接的技术指标要求,确保了星敏感器定标结果的可信度.

关键词:星敏感器;纳米分辨率;微调整;建模分析

中图分类号:V216.8 **文献标识码**:A **文章编号**:1004-4213(2017)10-1012004-9

Design of a Micro-adjustment Mechanism Used for Star Sensor Calibration Test

CHEN Qi-meng[1,2], ZHANG Guo-yu[1,2], ZHANG Jian[1], WANG Zhe[3], ZHANG Yu[4]

(1 *Department of Opto-Electronic Engineering, Changchun University of Science and Technology, Changchun* 130022, *China*)

(2 *Optical Measurement and Control Instrumentation, Jilin Province Engineering Research Center, Changchun* 130022, *China*)

(3 *Department of Science, Changchun University of Science and Technology, Changchun* 130022, *China*)

(4 *Key Laboratory of Space System Simulation, Beijing* 100000, *China*)

Abstract: Aiming at the practical requirements of accurate alignment between high-precision star sensor and the test equipment in ground calibration experiments, a nanoscale five-dimensional adjustment frame for calibration of star sensors is designed. The influence of optical axis alignment error on star sensor test was analyzed in detail. In order to ensure docking accuracy, the design idea of adopting the mechanical structure of stacked type was put forward. Then, the design scheme of a two-dimensional translation module and the three-dimensional adjustment module were discussed. After that, the simulation modeling and mechanical analysis of the adjustment frame were carried out. Finally, verification experiments were conducted on the designed micro-adjustment mechanism. The testing results show that, the displacement resolution can reach 25 nm, the angle resolution can reach 0.1 arcsecond; and the stability is quite high. Therefore, the designed micro-adjustment mechanism can meet the technical indicator requirements of accurate docking between star sensor and test equipment, and it can ensure calibration credibility of the star sensor.

Key words: Star sensor; Nanometer resolution; Micro-adjustment; Modeling analysis

OCIS Codes: 120.4820; 000.2170;150.1488;230.0230;350.5730

Foundation item: National Key Laboratory Fund Project in China (No.61420020210162002)

First author(Contact author): CHEN Qi-meng (1989—), female, lecturer, Ph. D. degree, mainly focuses on photoelectric instrument and calibration test technology of spacecraft. Email: qmchen1989@163.com

Received: Apr.7, 2017; **Accepted**: Jun.19, 2017

0 Introduction

With the rapid development of high-precision star sensors, the requirements for its ground test equipment are also getting higher and higher. In order toguarantee the calibration accuracy of a star sensor, it is very necessary to design a high precision, high stability matching equipment[1-5]. A multi-dimensional adjustment mechanism is the core equipment that can make the optical systems of a simulator and a sensor accurately docked in ground calibration experiment of a high-precision star sensor, and it is an important guarantee to realize high precision pick-up of simulated star point position and image information of a sensor. In order to meet the test requirements, there is an urgent need for a highly accurate five-dimensional adjustment mechanism to ensure the credibility of the calibration results. The efficiency and resolution of existing adjustment frames are relatively low[6-8]. During a calibration test, the pupil connection error between the star sensor and the calibration equipment is ± 1mm, and the optical axis docking error is 5 arcsecond, which increases the alignment error and reduces the test precision. In this paper, the influence of optical axis alignment error of an optical system on the test results of sensor precision was studied, and the necessity of designing a high-precision adjustment mechanism design was explained. What's more, the design process of high precision multi-dimensional adjusting mechanism was described in detail.

1 Calibration test principle of the star sensor and influence of optical axis consistency on the calibration results

1.1 Test principle for ground calibration of star sensors

Test principle for ground calibration of star sensors is shown in Fig. 1. When a micro-adjustment mechanism is working, the position of a star sensor head is adjusted by adjusting the micro-adjustment mechanism in order to realize a complete pupil docking with the star sensor and make the star sensor's optical axis be consistent with that of the micro-adjustment mechanism. Then, a piece of standard star point plate is placed on the focal plane of a collimating optical system of a simulator. After that, a beam of parallel light emits throughout the collimating optical system. Thus, we realize position simulation of fixed stars in fixed sky region from infinity and complete the ground calibration test for a star sensor.

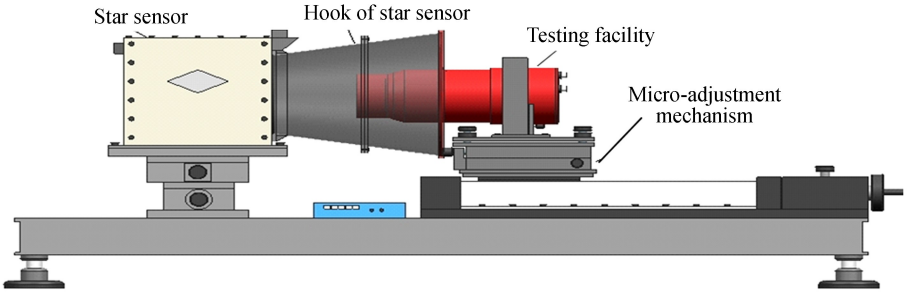

Fig.1 Test principle for ground calibration of star sensors

1.2 Influence of optical axis consistency on the calibration results

When using the micro-adjustment mechanism to adjust the position of thetest equipment, two basic elements should be ensured. The first is to ensure that all the star points of the full field of view emitting through the test equipment's optical system have the same luminous flux at the star sensor's entrance pupil, which requires that the exit pupil of the test equipment's optical system be consistent with the entrance pupil of the star sensor's optical system; the second is to try best to ensure that optical systems of the sensor and the test equipment are coaxial, which will improve accuracy and credibility of the calibration test.

There is an optical axis consistency error when the star sensor's optical system is docked with the test equipment's optical system. With a combination of the actual situation, optical axis consistency errors present in three forms, which are direction offset, tilt deviation, both direction offset and tilt deviation[9-11]. The three existence forms of optical axis consistency errors are as shown in Fig. 2, where Δl represents the direction offset and $\Delta\theta$ represents the inclination deviation value.

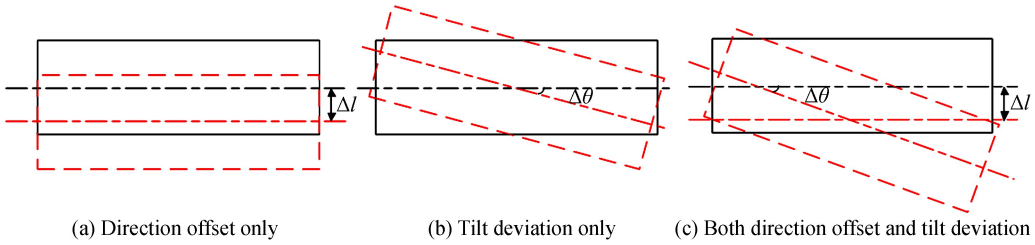

Fig.2 Three existence forms of optical axis consistency errors

The CCD detector of the star sensor receives the light emitting from the center of the test equipment′s optical axis, and the adjustment accuracy of the optical axis consistency is determined by the position of the bright spot on the target. The test principle is shown in Fig 3.

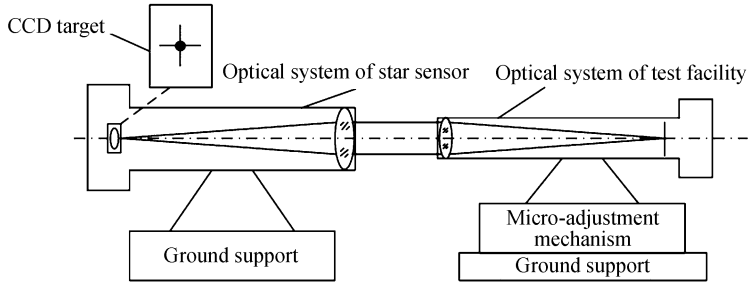

Fig.3 Accuracy test principle of optical axis consistency

The resolution θ of the star sensor′s CCD detector is related to the lattice size D of the CCD and the focal length f of the camera, that is $\theta = D/f$. In addition, the high-precision star sensor adopts pixel segmentation technology to extract target, the practical resolution can reach 1/8 of the original resolution. It is known that the lattice size of the star sensor′s CCD detector is 13μm and the focal length is 100mm. After calculation, we know that, if the star point at the center of the test equipment′s optical axis will image at the center of the CCD target, it is required to adjust micro-adjustment mechanism of a division value. The imaging position of the center star point on the CCD target moves, but does not exceed 3 ". Otherwise, no matter how to adjust the mechanism, it cannot make the imaging point accurately image at the center of the CCD target. Considering that the focal length f' of the collimating optical system of the test equipment and the angular resolution of the micro-adjustment mechanism should satisfy the following relation $\theta' \cdot f' \leq 1/8\theta \cdot f$. Therefore, only if the angle resolution of the adjustment mechanism reaches better than 0.5 arcsecond, can it make the test facility′s optical axis be consistent with the star sensor′s optical axis under the resolution of the CCD detector.

Whenthere is a position offset or an angle deviation between pupils of the test equipment and the star sensor, the light beams of simulated star points from the test equipment no longer all project into the entrance pupil of the star sensor, which will directly lead to the decrease of the test accuracy for magnitude; and along with the field of view increase, the simulated star points will lose more light energy. According to the pupil diameter of the high-precision star sensor, the quantitative analysis of the illumination change on receiving surface caused by pupil connection error is carried out. Fig. 4 shows the illumination change, where assuming that the position offset between the optical axes is 100μm and the angle deviation is 1 arcsecond.

Therefore, with a view to the above directions and operating requirements, the adjustment mechanism should not only have characteristics such as a certain adjusting range, a high resolution and high stability, but also should achieve respective precision adjustment on various directions (including X-Y translation, Z-axis translation, angles of pitch and azimuth). In addition, volume, mass and connection method must be seriously considered as well. Consequently, it is necessary to carry out well structural design and precise parameter calculation. According to the parameters of the star sensor and the test facility, the specifications of the micro-adjustment mechanism are determined and are shown in Table 1.

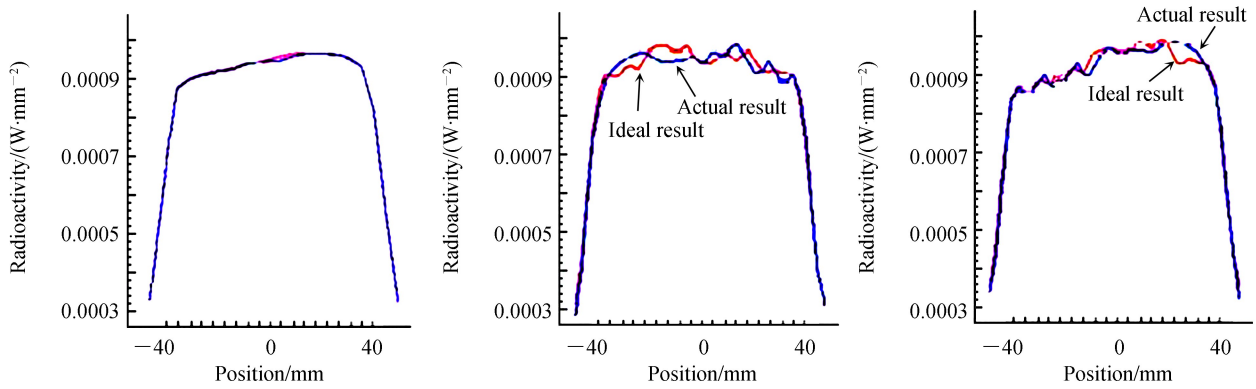

Fig.4 Illumination change on receiving surface caused by pupil connection error

Table1 Main technical parameters of the adjustment mechanism

Parameters	Target	
Adjusting range	Displacement±3 mm	Angle±1°
Resolution	Displacement 50 nm	Angle 0.3 arc second
Boundary dimension	≯210 mm×210 mm×120 mm	
Weight capacity	≯5 kg	

2 Mechanical structural design of the mechanism

The precision micro-adjustment mechanism features such as reliability and high resolution determine the adjustment precision of the optical axes directly which may affect the calibration results of sensors. So it is demanded that the high-precision adjustment mechanism should simultaneously be able to complete multi-dimension adjustments including horizontal movement, vertical movement and angular deflection. By using the combination structure form of stacked type, the adjustment mechanism is divided into two parts, which are X-Y two-dimension translation and θ_x, θ_y, Z three-dimension adjustment, to achieve multi-dimensional independent adjustment.

2.1 X, Y two-dimensional translation

When designing the mechanical system of X, Y two-dimensional translation, mechanical crawl should be avoided. Locate force points of X, Y driving components on the adjustment plate and use precision bearings at the contact parts to ensure the vertical precision of X-Y. The X-Y adjustment assembly structure and precise guiding mechanism structure schematics are shown in Fig.5. The motor is fastened to the screw by the coupling, the screw nut is fixed on a big wedge, and the big wedge is connected by the guide rail vice to a small wedge. The motor drives the screw to rotate and the screw flange along with the big wedge moves axially. However the small wedge can only move in radial direction due to axial limit of the shell, due to axial limit of the shell the adjustment of X, Y two-dimensional translation can be achieved.

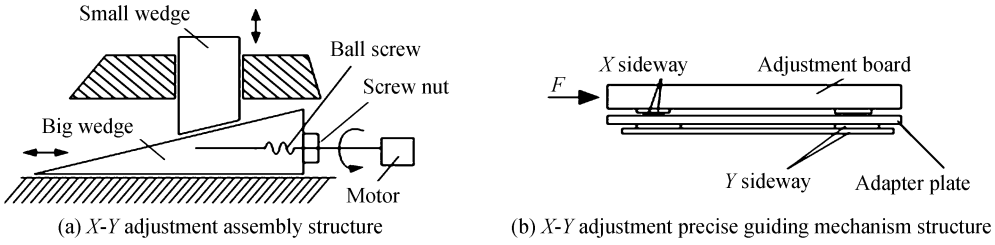

(a) X-Y adjustment assembly structure (b) X-Y adjustment precise guiding mechanism structure

Fig.5 X-Y adjustment assembly structure and precise guiding mechanism structure

2.2 θ_x, θ_y, Z three-dimensional adjustment

It is considered that using three similar Z adjustment components to avoid affects between one angle θ_x and the other angle θ_y during the adjustment. θ_x, θ_y, Z adjustment assembly structure and adjustment mechanism structure schematics are shown in Fig. 6. The motor is fastened to the screw by the coupling, the screw flange is fixed on the connector, and also is fastened to the big wedge through screw fastening as

well, and the big wedge is connected to the small wedge through the guide rail vice. The motor drives the screw to rotate and the screw flange along with the big wedge moves axially. However the small wedge can only move in Z-axis radial direction due to the limit from the baffle limit. Therefore, the adjustment of Z-axis translation can be achieved by contacting the small wedge to the adjustment plate through the ejector pin.

The three mandrels contacting to the adjustment plate formed three points, which may form an isosceles right triangle. Then the isosceles right triangle together with the draw springs consist a structure of three tight-three pull. Each right angle side of the triangle is a rotating axis. In this way, it can achieve the result that when adjusting one angle θ_x, the other one θ_y is not affected. Consequently, the vertical adjustment Z-axis translation as well as the angle adjustment of θ_x and θ_y can be achieved.

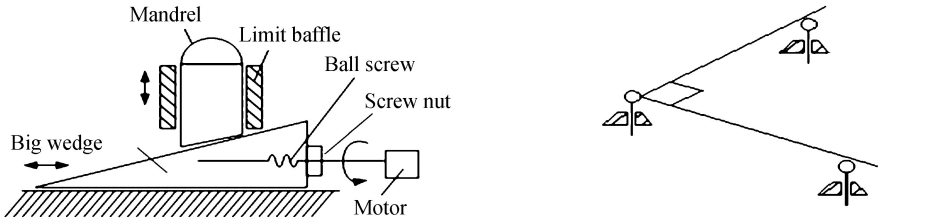

Fig.6 θ_x, θ_y, Z adjustment assembly structure and adjustment mechanism structure

3 Three-dimensional modeling and mechanical analysis

3.1 Three-dimensional modeling of the mechanism

The assembly relationship and displacement drive structures of X, Y two-dimensional translation are shown in Fig.7. The displacement drive components shall be placed into the rectangular groove of the shell and it is connected with the bottom plate through a linear guide under the big wedge. The motor drives the screw to spin, the two wedges move by virtue of the linear guide sliding block, and the small wedge can only do radial displacement.

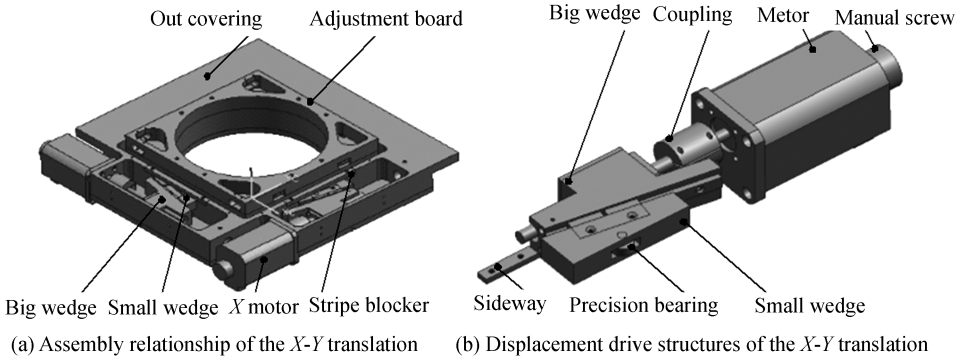

Fig.7 Assembly relationship and displacement drive structures of X-Y translation

The assembly relationship and adjustment drive structures of θ_x, θ_y, Z three-dimensional adjustment are shown in Fig. 8. The adjustment drive structure is connected to the surface of the Z-layer fixing plate by means of a linear guide and a motor fixing plate. The motor drives the screw to spin and the flange block drives the big wedge to move; while the axial movement of the small wedge is limited by the baffle, the two wedges move by virtue of the linear guide, and then the movement of the Z adjustment plate can be controlled by the mandrels.

After assembling the complete Three-dimensional model for the designed adjustment mechanism, and the overall three-dimension model is shown in Fig. 9, we come to the conclusion that the micro-adjustment mechanism contains the excellent characteristics such as a symmetrical structure, a compact arrangement, a hollow inner structure and a light weight.

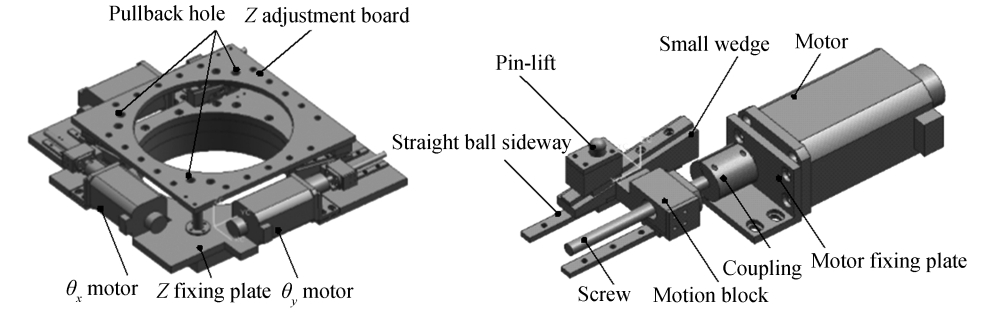

(a) Assembly relationship of the θ_x, θ_y, Z adjustment (b) Adjustment drive structures of the θ_x, θ_y, Z adjustment

Fig.8 Assembly relationship and adjustment drive structures of θ_x, θ_y and Z adjustment

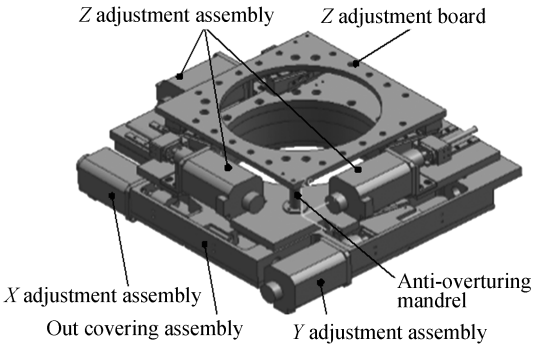

Fig.9 Overall three-dimensional model

3.2 Mechanical analysis

The Mechanical analysis of the multidimensional adjustment mechanism is simplifying the key components into abstract elastomers, and using the finite element method to get the analysis results, and then verifying the design rationality of the key components.

Regarding the force of any position on the object as two orthogonal forces, we respectively name the normal stress of three directions x, y, z as σ_x, σ_y, σ_z, and name the shear stress of three directions as τ_{xy}, τ_{yz}, τ_{zx}. Then, we use the vector method to express the composition of forces as

$$\boldsymbol{\sigma}=[\sigma_x,\sigma_y,\sigma_z,\tau_{xy},\tau_{yz},\tau_{zx}] \tag{1}$$

Assuming that the strain of any point on the elastic body is represented by the positive strain ε_x, ε_y, ε_z and the shear strain γ_{xy}, γ_{yz}, γ_{zx}, and the strain matrix is expressed as

$$\boldsymbol{\varepsilon}=[\varepsilon_x,\varepsilon_y,\varepsilon_z,\gamma_{xy},\gamma_{yz},\gamma_{zx}]^{\mathrm{T}} \tag{2}$$

Then the equilibrium equation of the three-dimensional model is expressed as

$$\begin{cases}\dfrac{\partial\sigma_x}{\partial x}+\dfrac{\partial\sigma_{yz}}{\partial y}+\dfrac{\partial\sigma_{zx}}{\partial z}+\overline{f_x}=0\\ \dfrac{\partial\tau_{xy}}{\partial x}+\dfrac{\partial\tau_y}{\partial y}+\dfrac{\partial\tau_{zx}}{\partial z}+\overline{f_y}=0\\ \dfrac{\partial\tau_{xy}}{\partial x}+\dfrac{\partial\tau_{yz}}{\partial y}+\dfrac{\partial\tau_z}{\partial z}+\overline{f_z}=0\end{cases} \tag{3}$$

$\overline{f_x}$, $\overline{f_y}$ and $\overline{f_z}$ are the components of the unit volume in the direction of x, y, z.

And the geometric equation of the three-dimensional model is expressed as

$$\begin{cases}\varepsilon_x=\dfrac{\partial u}{\partial x},\varepsilon_y=\dfrac{\partial v}{\partial y},\varepsilon_z=\dfrac{\partial w}{\partial z}\\ \gamma_{xy}=\dfrac{\partial u}{\partial y}+\dfrac{\partial v}{\partial x}=\gamma_{yx}\\ \gamma_{yz}=\dfrac{\partial v}{\partial z}+\dfrac{\partial w}{\partial y}=\gamma_{zy}\\ \gamma_{zx}=\dfrac{\partial u}{\partial z}+\dfrac{\partial w}{\partial x}=\gamma_{xz}\end{cases} \tag{4}$$

According to the above mechanical analysis, we apply the gravitational load to the overall structure of the adjustment mechanism and the support frame, the analysis results of the self-weight deformation are shown in Fig. 10. The results show that the maximum deformation of the adjustment mechanism is located on the clamping structure of the test equipment's optical system, not on the adjustment mechanism itself. Therefore it will not change any performance of the test equipment, and it may guarantee test accuracy of the test equipment.

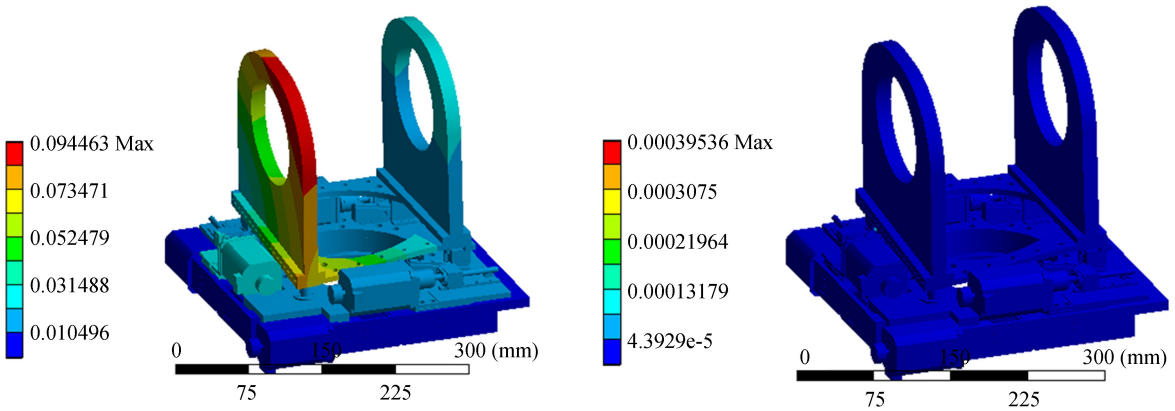

(a) Self-weight deformation map of the adjustment mechanism (b) Self-weight deformation map of the support frame

Fig.10 Self-weight deformation map of the adjustment mechanism and the support frame

4 Resolution calculation and test results

4.1 Resolution calculation

Parameters of the choice products used on micro-adjustment mechanism are as follows: the motor's reduction ratio is 1:50 and step angle is 1.8°, the angle of wedge is $\theta=10°$, the route distance of big wedge is $l'=40$ mm. There are three mandrels connecting three support points of the assemblies on Z-axis. The three support points constitute a right triangle with length of side 80 mm. Then the displacement resolution l, the displacement range L, the angular resolution θ' and the angular range Ψ of the adjusting mechanism are given in the following formulas,

$$l=(1.8°/50)\times\frac{1}{360}\times\tan\theta\times10^6=17.6\ \text{nm} \tag{5}$$

$$L=l'\times10°=9.64\ \text{mm} \tag{6}$$

$$\theta'=\arctan(l/80)\times3600=0.045'' \tag{7}$$

$$\Psi=\arctan(L/80)=6.87° \tag{8}$$

The results show that: through a multi-level segmentation, the linear displacement resolution of the micro-adjustment mechanism can achieve nanometer scale on X, Y, Z axes, and angle displacement resolution can achieve sub-second scale on θ_x and θ_y. Thus the designed adjustment mechanism can precisely adjust the facilities during the calibration test of the star sensor.

4.2 Test experiment and test results

4.2.1 Resolution test of the micro-adjustment mechanism

Fig. 11 shows the test photo of a micro-adjustment mechanism, the resolution and the stability are tested by a ZYGO interferometer. Firstly we put the five-dimensional adjustment mechanism on the interferometer's own three-dimensional adjustment stage. Then we put a high-precision standard spherical mirror on the Z adjustment plate of the adjustment mechanism through a adapter. Before using the interferometer

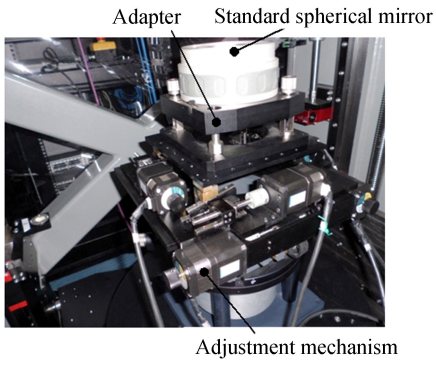

Fig.11 Test photo of micro-adjustment mechanism

to test the resolution and stability, the initial position should be determined first. The horizontal position is generally selected as the initial position, where the interference fringe is the center bright spot. After that, we adjust the adjustment mechanism′s five degrees of freedom and observe the value changes of the fringe data on the computer interface. Finally, we get test results of resolution and stability.

Test results and conclusions: The linear displacement resolution is 25 nm on X, Y, Z axes and the theoretical value is 17.6 nm; the angle resolution is 0.1 arcsecond on θ_x, θ_y and the theoretical value is 0.045 arcsecond. So it is further verified that the designed adjustment mechanism can totally meet the docking precision requirements of the calibration test.

4.2.2 Calibration test of high-precision star sensor

Star point position test is carried out on the star map after equipment installation. Then, we read pitch angle and azimuth of each star point. After that, we calculate the actual position of each star point. At last, we describe the position by angle degree and compare the results with theoretical ones. The actual angular distance value and error value are given in the following formulas,

$$\gamma_{\text{actual}} = \arccos\left[\cos\beta_i \cos\beta_j \cos(\alpha_i - \alpha_j) + \sin\beta_i \sin\beta_j\right] \tag{9}$$

$$\Delta = (\gamma_{\text{actual}} - \gamma_{\text{theoretical}}) \times 3600'' \tag{10}$$

As is shown inFig. 12, all the angular distance errors between stars are less than 10″. The error distribution diagram illustrates that the calibration precision is improved by using the micro-adjustment mechanism. The test results are superior to those results by using normal adjustment mechanism. Among all errors, the maximum data is 11.02 arcsecond which can meet the parameters demand of the calibration test of high-precision star sensor.

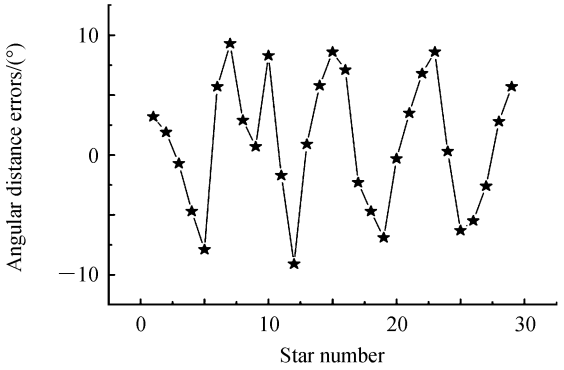

Fig.12 Angular distance errors

5 Conclusion

Focusing on the influence factors of the accuracy index of high-precision star sensor′s ground calibration test, a nanoscale micro-adjustment mechanism used in calibration test for high-precision star sensor was designed. We analyze the influence of optical axis consistency between the test equipment and the star sensor on the key parameter test results; deeply study the structure of the adjustment mechanism and the design scheme of each component; carry out simulated analysis and resolution calculation on the test results. The experimental results show that the actual linear displacement resolution and the angle displacement resolution are both very high. They are respectively 25nm on X, Y, Z axes and 0.1 arc second on θ_x, θ_y. In addition, the test equipment supported by the designed five-dimension adjustment mechanism was very stable during the whole test process and the precision of the star position was quite high. All angular distance errors between stars are better than 10 arcsecond, which can satisfy the calibration test requirements for high- precision star sensor.

References

[1] MENG Yao, ZHANG Guo-yu, SUN Gao-fei, *et al*. Optical system of high contrast dynamic star simulator based on LCOS splicing technology[J]. *Optics and Precision Engineering*, 2016, **24**(3): 511-520.

[2] WANG Ling-yun, WANG Bo, ZHANG Guo-yu, *et al*.Star point energy center crrection method of star simulator [J]. *Acta Photonica Sinica*,2016,**45**(2):0223001.

[3] SUN Xiang-yang,ZHANG Guo-yu, DUAN Jie, *et al*. Design of star charts simulator for high-precision star simulator [J]. *Acta Optica Sinica*, 2012,**32**(5): 0523001.

[4] GAO Yun-guo, ZHANG Qian, SHI Ya-li, *et al*. Structure design of precise displacement platform without guiding apparatus [J]. *Optics and Precision Engineering*, 2009, **17**(9):2199-2204.

[5] LUO Yong. Coordinates-decoupling of multidimensional precision optical adjusting frame [J]. *Opto-Electronic Engineering*, 2011, **38**(4):37-40.

[6] BERANEK M W,CHAN E Y,CHEN C C, *et al*. Passive alignment optical subassemblies for military/aerospace fiber-optic transmitter receiver applications [C]. IEEE Proceedings,49th Electronic Components and Technology Conference,

San Diego, CA, USA, Jun 1-4, 1999:188-196.

[7] CHEN Yong. Machine design and calculation of optical precision mount with large- aperture [J]. machine building & automation, 2005, **34**(2):23-25, 28.

[8] TOSU K, HAGA Y, ESASHIM. Three-axis magneto-impedance effect sensor system for detecting position and orientation of catheter tip [J]. *Sensors and Actuators*, 2004, (A111):304-309.

[9] ZHAO Chen-guang, TAN Jiu-bin, LIU Jian, *et al*. Star simulator for testing celestial navigation equipment [J]. *Optics and Precision Engineerin*, 2010,**18**(6):1326-1332.

[10] LIU Ya-ping,LI Juan,ZHANG Hong. Design and calibration of star simulator [J]. *Infrared and Laser Engineering*, 2006,**10**(35): 24-28.

[11] LIU Shi, ZHANG Guo-yu, SUN Gao-fei, *et al*. Design of high-presition static star simulator with uniform sky background [J]. *Acta Photonica Sinica*, 2016,**45**(12):1222002.